

Fig. 4 Sail steering angles (—, cone angle, ---, clock angle).

For a large number of trajectory segments, the transfer time is extremely close to the true minimum time, as expected. However, for a small number of segments there is only a modest penalty, as shown in Table 1. For example, using four fixed-sail attitudes during the entire trajectory the transfer time is increased by only 10 days. The trajectory obtained is shown in Fig. 1 while the steering angles are shown in Fig. 2. It can be seen that for a larger number of segments the steering law closely matches that obtained from the Pontryagin principle.

This approach can now be extended to rendezvous trajectories. For illustration a three-dimensional Earth–Mars transfer problem will be considered. A launch date of 13 May 1986 is chosen to allow comparison with the existing analysis of Sauer.² The minimum transfer time obtained from the Pontryagin principle is found to be 355.7 days. Again using sequential quadratic programming to minimize the transfer time while enforcing the boundary conditions as constraints, the transfer time using fixed steering angles is found to be 365.0 days for $N = 5$. For $N = 10$ the transfer time is reduced slightly to 362.0 days. The three-dimensional rendezvous trajectory to Mars capture obtained with $N = 5$ is shown in Fig. 3, whereas the sail steering angles are shown in Fig. 4. For three-dimensional transfers the sail clock angle is also required, defined to be the angle between the north ecliptic pole and a projection of the sail normal onto a plane normal to the sun line. Again, the ease of implementing only five fixed steering angles, rather than continuously tracking the true minimum-time steering angles, will more than offset the modest increase in transfer time.

IV. Conclusions

An investigation has been conducted into near minimum-time solar-sail trajectories. Using the observation that the cost function of the problem is rather flat means that near minimum-time trajectories can be obtained using only simple steering laws. Although these steering laws incur a modest penalty in transfer time, they are likely to provide significant operational benefits, particularly for future highly autonomous missions. Because solar sails do not require reaction mass, absolute trajectory optimization is of less importance than for other low-thrust spacecraft.

References

- ¹McInnes, C. R., *Solar Sailing: Technology, Dynamics and Mission Applications*, Springer-Verlag, London, 1999, pp. 19–29.
- ²Sauer, C. G., “Optimum Solar Sail Interplanetary Trajectories,” AIAA Paper 76-792, Aug. 1976.
- ³McFarland, C. A., and Leipold, M., “Mainbelt Asteroid Rendezvous Missions Using Solar Electric and Solar Sail Propulsion,” American Astronautical Society 96-167, Feb. 1996.
- ⁴Van der Ha, J. C., “The Attainability of the Heavenly Bodies with the Aid of a Solar Sail,” German Society for Aeronautics and Astronautics, DGLR Paper 80-012, March 1980.

Model Correction for Sampled-Data Models of Structures

S. O. Reza Moheimani*

University of Newcastle,

Newcastle, New South Wales 2308, Australia

I. Introduction

THE modal analysis technique¹ has been extensively used throughout the literature to model dynamics of distributed systems such as flexible beams and plates, slewing beams, piezoelectric laminate beams, and acoustic ducts. Dynamics of such systems are described by partial differential equations (PDEs). In the modal analysis approach, the solution of these PDEs is allowed to consist of an infinite number of terms. Moreover, these terms are chosen to be orthogonal. Hence, modeling of a system based on a modal analysis approach can result in an infinite-dimensional model of that system.

In control design problems, one is often interested only in designing a controller for a particular frequency range. In these situations, it is common practice to remove the modes that correspond to frequencies that lie out of the bandwidth of interest and only keep the modes that directly contribute to the low-frequency dynamics of the system. Often two or more out-of-bandwidth modes may also be kept to improve the in-bandwidth model of the structure.

It is known that truncation has the potential to perturb the in-bandwidth zeros of the system. This problem is addressed in Ref. 2 and was recently revisited in Refs. 3 and 4. The mode acceleration method (see Ref. 2 page 350, and also Ref. 3) is concerned with capturing the effect of higher-frequency modes on the low-frequency dynamics of the system by adding a zero-frequency term to the truncated model to account for the compliance of the ignored modes. In Ref. 5, this problem is approached from an optimization perspective, where the DC content of the truncated model is modified to minimize the \mathcal{H}_2 norm of the error system that results from the truncation. In this paper, we concentrate on the sampled-data models of structures that are obtained by placing a sample and hold in the input of the system. We allow for a zero-frequency term to capture the effect of truncated modes and find this constant term such that the \mathcal{H}_2 norm of the resulting error system is minimized.

To this end, we point out that there are alternative methods to the modal analysis approach for modeling of distributed systems. However, the modal models have the interesting property that they describe spatial and temporal behavior of a system. Such models can then be used in designing spatial controllers as noted in Refs. 6 and 7.

II. Model Correction

Dynamics of a large number of distributed systems such as flexible beams, plates, and acoustic enclosures are governed by particular PDEs. Very often modal analysis is used, to solve these PDEs.¹ When modal analysis is used, a PDE can be shown to be equivalent to an infinite number of decoupled second-order, ordinary differential equations as

$$\ddot{q}_i(t) + \omega_i^2 q_i(t) = F_i u(t), \quad i = 1, 2, \dots \quad (1)$$

where $u(t)$ is the input of the system and q_i , $i = 1, 2, \dots$, are the modal coordinates. Moreover, the input–output equation of the system in terms of a transfer function can be shown to be

$$G(s, r) = \sum_{i=1}^{\infty} \frac{\phi_i(r) F_i}{s^2 + \omega_i^2} \quad (2)$$

Received 21 January 2000; revision received 20 October 2000; accepted for publication 9 November 2000. Copyright © 2001 by the American Institute of Aeronautics and Astronautics, Inc. All rights reserved.

*Senior Lecturer, Department of Electrical and Computer Engineering and the Centre for Integrated Dynamics and Control; reza@ee.newcastle.edu.au.

where $\phi_i(r)$, $i = 1, 2, \dots$, are mode shapes of the system. We are mainly concerned with pointwise models of structures. For controller design purposes, these models are often truncated by keeping the first N modes that lie within the bandwidth of interest. Truncation is known to perturb the in-bandwidth zeros of the system. In particular in the collocated case, when the actuator and sensor are located in the same position, this effect is easily observable.

Let us consider a structural model defined by

$$G(s) = \sum_{i=1}^{\infty} \frac{F_i}{s^2 + \omega_i^2} \quad (3)$$

To implement a controller, a sample and hold circuit is placed at the input to the system. This is to ensure that the system can be controlled via a computer. A sampled-data model of this system is determined by

$$G(z) = \mathcal{Z} \left\{ \frac{1 - e^{-Ts}}{s} \times \sum_{i=1}^{\infty} \frac{F_i}{s^2 + \omega_i^2} \right\} \quad (4)$$

where $\mathcal{Z}\{F(s)\}$ is the z transform of $F(s)$ and T is the sampling time. It can be shown that

$$G(z) = \sum_{i=1}^{\infty} \frac{F_i(1 - \cos \omega_i T)}{\omega_i^2} \times \frac{z + 1}{z^2 - 2 \cos \omega_i T z + 1} \quad (5)$$

In a typical controller design scenario, this model is then approximated by $G_N(z)$ by keeping the first N modes of Eq. (5) and a controller is designed based on the truncated model. That is,

$$G_N(z) = \sum_{i=1}^N \frac{F_i(1 - \cos \omega_i T)}{\omega_i^2} \times \frac{z + 1}{z^2 - 2 \cos \omega_i T z + 1} \quad (6)$$

The assumption that is made in truncation is that only the first N modes are of importance as far as the low-frequency dynamics of the structure is concerned. The fact is, however, that truncated modes do contribute to the low-frequency dynamics of the system. In particular, the DC contribution of the truncated modes is

$$\sum_{i=N+1}^{\infty} \frac{F_i}{\omega_i^2} \quad (7)$$

This error manifests itself in the form of perturbed zeros. One could attempt to reduce this error by adding Eq. (7) to the truncated model (6). This problem was addressed by Clark³ for continuous-time models of structures and a similar model correction technique was proposed (see also Ref. 8). Note that for sampled-data models a similar result can be obtained. This is because sampling does not alter the DC behavior of a system.

The problem that we wish to address in this paper is to find a model correction term K such that the corrected truncated model

$$\hat{G}_N(s) = \sum_{i=1}^N \frac{F_i(1 - \cos \omega_i T)}{\omega_i^2} \times \frac{z + 1}{z^2 - 2 \cos \omega_i T z + 1} + K \quad (8)$$

is as close to Eq. (5) as possible in an \mathcal{H}_2 sense. This is equivalent to finding a K that minimizes the following cost function:

$$\|W(z)(G(z) - \hat{G}_N(z))\|_2^2 \quad (9)$$

where $W(z)$ is an ideal low-pass filter with a cutoff frequency of ω_c and

$$\|f(z)\|_2^2 = \frac{1}{2\pi} \int_{-\pi}^{\pi} f^*(e^{j\omega}) f(e^{j\omega}) d\omega$$

The cost function (9) can be written in the form

$$\left\| W(z) \left(\sum_{i=N+1}^{\infty} G_i(z) - K \right) \right\|_2^2 \quad (10)$$

where

$$G_i(z) = \frac{F_i(1 - \cos \omega_i T)}{\omega_i^2} \times \frac{z + 1}{z^2 - 2 \cos \omega_i T z + 1}, \quad i = 1, 2, \dots$$

Let us define

$$\bar{G}(z) = \sum_{i=N+1}^{\infty} G_i(z) \quad (11)$$

Then the cost function (10) can be expanded as

$$\begin{aligned} \|W(z)(\bar{G}(z) - K)\|_2^2 &= \|W(z)\bar{G}(z)\|_2^2 - \langle W(z)\bar{G}(z), \\ &W(z)K \rangle - \langle W(z)K, W(z)\bar{G}(z) \rangle + \|W(z)K\|_2^2 \end{aligned}$$

where

$$\langle f, g \rangle = \frac{1}{2\pi} \int_{-\pi}^{\pi} f^*(e^{j\omega}) g(e^{j\omega}) d\omega$$

It can be verified that the K that minimizes Eq. (10) is given by

$$K_{\text{opt}} = \frac{\langle \bar{G}W, W \rangle + \langle W, \bar{G}W \rangle}{2\|W\|_2^2} \quad (12)$$

That is,

$$\begin{aligned} K_{\text{opt}} &= \frac{1}{2\omega_c} \int_{-\omega_c T}^{\omega_c T} \{ \bar{G}(e^{j\omega}) + \bar{G}^*(e^{j\omega}) \} d\omega \\ &= \frac{1}{2\omega_c} \int_{-\omega_c T}^{\omega_c T} \sum_{i=N+1}^{\infty} \frac{F_i(1 - \cos \omega_i T)}{\omega_i^2} \\ &\quad \left\{ \frac{e^{j\omega} + 1}{e^{j2\omega} - 2 \cos(\omega_i T) e^{j\omega} + 1} \right. \\ &\quad \left. + \frac{e^{-j\omega} + 1}{e^{-j2\omega} - 2 \cos(\omega_i T) e^{-j\omega} + 1} \right\} d\omega \\ &= \frac{1}{2\omega_c} \int_{-\omega_c T}^{\omega_c T} \sum_{i=N+1}^{\infty} \frac{F_i(1 - \cos \omega_i T)}{\omega_i^2} \times \frac{1 + \cos \omega}{\cos \omega - \cos \omega_i T} d\omega \end{aligned} \quad (13)$$

After straightforward, but tedious, manipulations, this expression for K_{opt} can be simplified to

$$\begin{aligned} K_{\text{opt}} &= \sum_{i=N+1}^{\infty} \frac{F_i(1 - \cos \omega_i T)}{\omega_i^2} \left\{ 1 + \frac{1}{2\omega_i T} \cot \frac{\omega_i T}{2} \ell_n \right. \\ &\quad \left. \times \left[\frac{\tan(\omega_i T/2) + \tan(\omega_c T/2)}{\tan(\omega_i T/2) - \tan(\omega_c T/2)} \right] \right\} \end{aligned} \quad (14)$$

We notice that, for large values of ω_i , the argument of the sum in (14) approaches zero. Therefore, to compute a reasonably accurate value for K_{opt} , one only needs to evaluate the sum for a large number of terms.

To this end, we point out that the preceding analysis does not consider the effect of modal damping. However, the correction term given in Eq. (14) should work well if a small amount of damping is allowed in model (3). The example in the next section illustrates this point. Therefore, this method should work fine for lightly damped systems. For a stiff structure the preceding analysis may have to be redone to allow for damping explicitly in model (3). In that case, one may need to perform the entire procedure numerically because finding an analytical solution may prove to be too tedious.

III. Illustrative Example

In this section, we apply the approximation mechanism developed in Sec. II to a simple flexible structure. The structure consists of a flexible beam that is pinned at its both ends. The beam is assumed to be subject to a point force at the point r_1 and a displacement sensor is assumed to be placed at r_2 . Parameters of the beam are beam length $L = 1.3$ m, actuator location $r_1 = 0.075$ m, sensor location $r_2 = r_1$, $\rho A = 0.6265$ kg/m, and $EI = 5.329$ Nm², where E , I , A , and ρ are, respectively, Young's modulus, moment of inertia, cross-sectional area, and the linear mass density of the beam.

Here, we assume that the system input is a point force applied at position r_1 and that the output is the displacement measured at

position r . The transfer function between applied force u and the elastic deflection of the beam can be shown to be

$$\frac{\hat{y}(s, r)}{U(s)} = \sum_{i=1}^{\infty} \frac{\phi_i(r_1)\phi_i(r)}{(s^2 + \omega_i^2)} \tag{15}$$

For the pinned–pinned beam system, the mode functions are given by¹

$$\phi_i(r) = \sqrt{(2/\rho AL)} \sin(i\pi r/L) \tag{16}$$

and the corresponding natural frequencies are

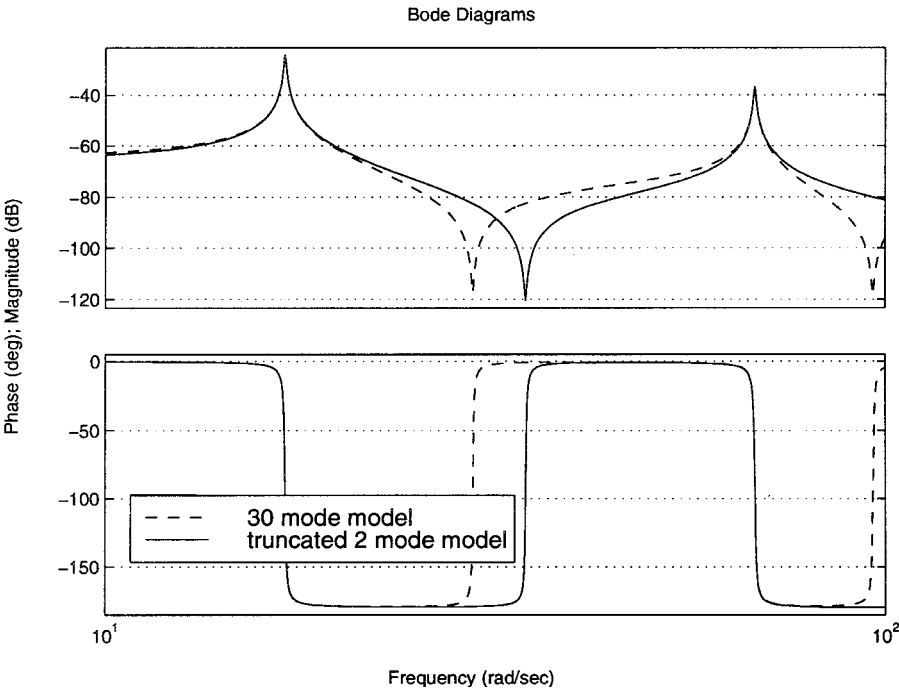


Fig. 1 Comparison of the frequency responses of the 30-mode sampled-data model of the beam with its 2-mode sampled-data model.

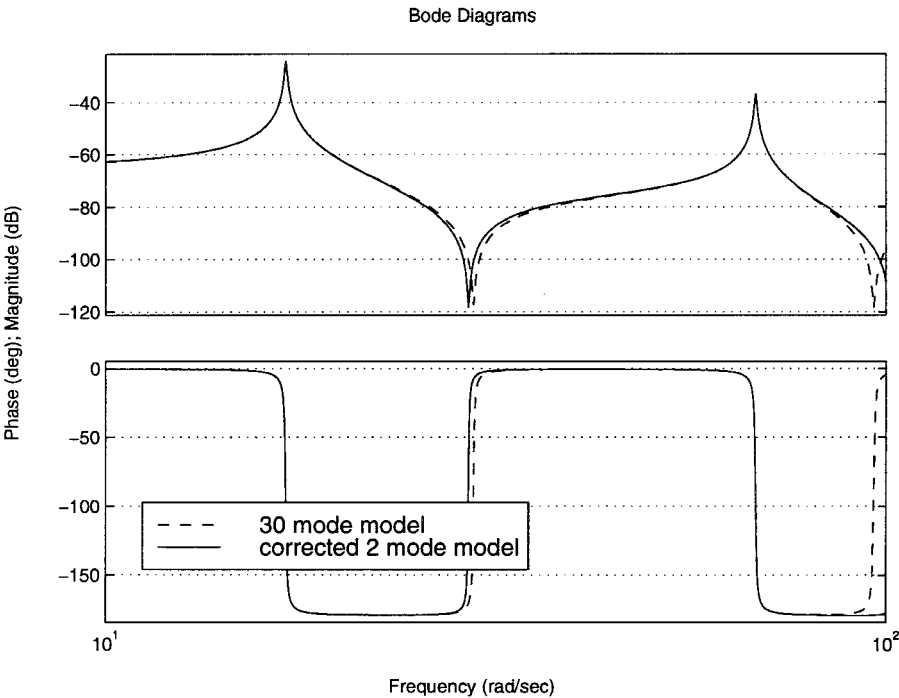


Fig. 2 Comparison of the frequency responses of the 30-mode sampled-data model of the beam with its corrected 2-mode sampled-data model.

$$\omega_i = (i\pi/L)^2 \sqrt{EI/\rho A}$$

This system consists of an infinite number of modes, and it describes the elastic deflection of the entire beam due to a point force applied at r_1 . Because the actuator and the sensor are located at the same position, this is a collocated system.

In this example, we assume that the system is sampled at a rate of $T = 0.1$ ms. Moreover, we assume that all of the modes have a damping ratio of 0.3%. In Fig. 1, we compare the frequency response of the two-mode sampled-data model of the beam and the model based on the first 30 modes. Note that truncation has considerably perturbed the zeros of the two-mode truncated model. In Fig. 2, we plot the corrected version of the two-mode system based on the procedure developed in the Sec. II, that is using Eq. (14). The correction term, K_{opt} captures the effect of modes 3–30 on the two-mode dynamics of the system in a \mathcal{H}_2 optimal sense. Note that the corrected 2-mode system approximates the 30-mode system reasonably well in the frequency range of interest.

IV. Conclusions

In this paper we looked at the problem of model correction for sampled data models of flexible structures. The problem of finding a feed-through term to compensate for the effect of truncated higher-frequency modes on in-bandwidth dynamics of the system was set up as an \mathcal{H}_2 optimization problem and an analytical solution to this problem was obtained.

Acknowledgment

This work was supported by the Australian Research Council.

References

- ¹Meirovitch, L., *Elements of Vibration Analysis*, 2nd ed., McGraw-Hill, Sydney, 1986, Chap. 6.
- ²Bisplinghoff, R. L., and Ashley, H., *Principles of Aeroelasticity*, Dover, New York, 1962.
- ³Clark, R. L., "Accounting for Out-of-Bandwidth Modes in the Assumed Modes Approach: Implications on Collocated Output Feedback Control," *Journal of Dynamic Systems, Measurement, and Control*, Vol. 119, Sept. 1997, pp. 390–395.
- ⁴Zhu, X., and Alberts, T. E., "Appending a Synthetic Mode to Compensate for Truncated Modes in Collocated Control," *Proceedings of the AIAA Guidance, Navigation, and Control Conference*, AIAA, Reston, VA, 1998.
- ⁵Moheimani, S. O. R., "Minimizing the Effect of Out of Bandwidth Modes in Truncated Structure Models," *Journal of Dynamic Systems, Measurement, and Control*, Vol. 122, March 2000, pp. 237–239.
- ⁶Moheimani, S. O. R., Petersen, I. R., and Pota, H. R., "Broadband Disturbance Attenuation over an Entire Beam," *Journal of Sound and Vibration*, Vol. 227, No. 4, 1999, pp. 807–832.
- ⁷Moheimani, S. O. R., Pota, H. R., and Petersen, I. R., "Spatial Balanced Model Reduction for Flexible Structures," *Automatica*, Vol. 35, No. 2, 1999, pp. 269–277.
- ⁸Wilson, E. L., Yuan, M., and Dickens, J. M., "Dynamic Analysis by Direct Superposition of Ritz Vectors," *Earthquake Engineering and Structural Dynamics*, Vol. 10, 1982, pp. 813–821.